report for analysis

Kazuhiro Ishikawa

December 22, 2003

Contents

1 beam line detector analysis

1.1 timing calibration for TDC at RF,plastic scintillator,PPAC

1.1.1 summary

We should get physical information from the obtained data,digital data taken by the data acquisition system. In this section, I analyze timing calibration of F2PL,RF and PPAC.

1.1.2 ch⇔ns

In following a picture, this is a raw data of timing signals which correspond to the time arranged to the 20 ns.

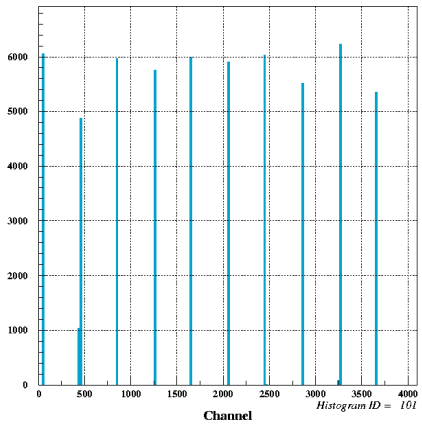

Figure 1: tdc ch

To convert obtained digital data to ns, I used following function.

$$\mathrm{T(ns)} = \mathrm{aX(ch)} + \mathrm{b} \tag{1}$$

h

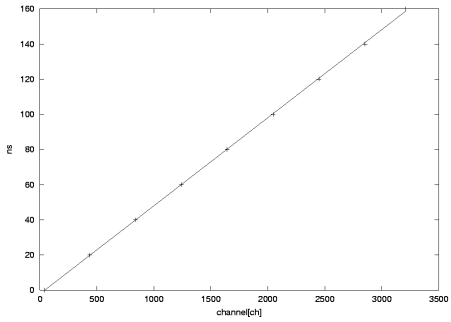

Figure 2: tdc ch

h

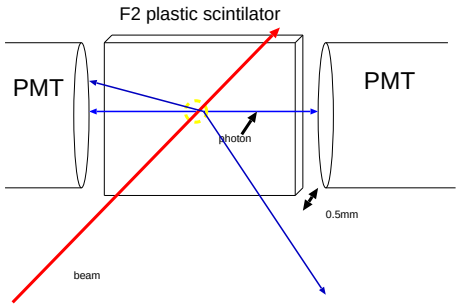

Figure 3: tdc ch

1.2 RIPS and plastic scintillator

1.2.1 summary

F2PL has mainly purpose of two parts. One part is for particle identity of the beam from RIPS. And another part is to measure TOF ,time of flight for calculating a momentum of the beam. The relay of this TOF is that of from F0 to F2.

1.2.2 principle

This section is an introduction for how to do a particle identity. In magnetic filed ,D1 and D2 ,the motion of charged particle is Lorenz motion and thus, following equation is concluded for charged particle.

- B:value of magnetic filed
- ρ:radius of curvature

- Z:number of proton of charged particle
- A:number of mass of charged particle

$$B\rho \propto \frac{A}{Z} \tag{2}$$

This shows that the particle is separated if $\frac{A}{Z}$ of the particle is different. The equation of the energy loss of a charged particle which passes though a matter is given by following .

- v:velocity of charged particle
- TOF: time of flight of certain section

$$\Delta E \propto \frac{Z^2}{v^2} = Z^2 \mathrm{tof}^2 \tag{3}$$

This shows that I can separate the particles which are different number of Z.This part is done by Al degrader which is between D1 and D2. If I modify the magnetic filed value of D2 which is fits to the particle which is used in this experiment, the particle far from ones is rejected because of different proton number by using degrader composed of Al between D1 and D2 which caused different energy loss ,thus changing particle velocity. So I can select particles which are around the ones which is used in this experiment. But this mixes other particles around that which is not to be able to separate in Rips. To reject that, I use a F2PL.This gives me timing signal and pulse height caused by charged particle passing though that material. I can do the identify the particle by equation 3.

1.2.3 calibration beam^{25}Ne and particle identity

For purpose of following calibration, I used the run which is ^{25}Ne. That has $\Delta p/p = \pm 0.1\%$,the momentum of distribution. Before calibration, I must select ^{25}Ne by using the correlation between pulse height of F2PL and TOF from F0 to F2PL. To identify the particle. I reefer the simulation code ,Intensity. This gives me intensity of various fragment which goes from RIPS and above correlation on simulation.

1.2.4 slew correction of the plastic scintillator

By the threshold of a discriminator, the timing of low pulse height on analog signal is delayed compared to other region of energy. To correct the slew signal, I used following equation.

$$< A >= \frac{a}{T^b} \tag{4}$$

Figure 4: TOF vs ΔE from calculation of Intensity

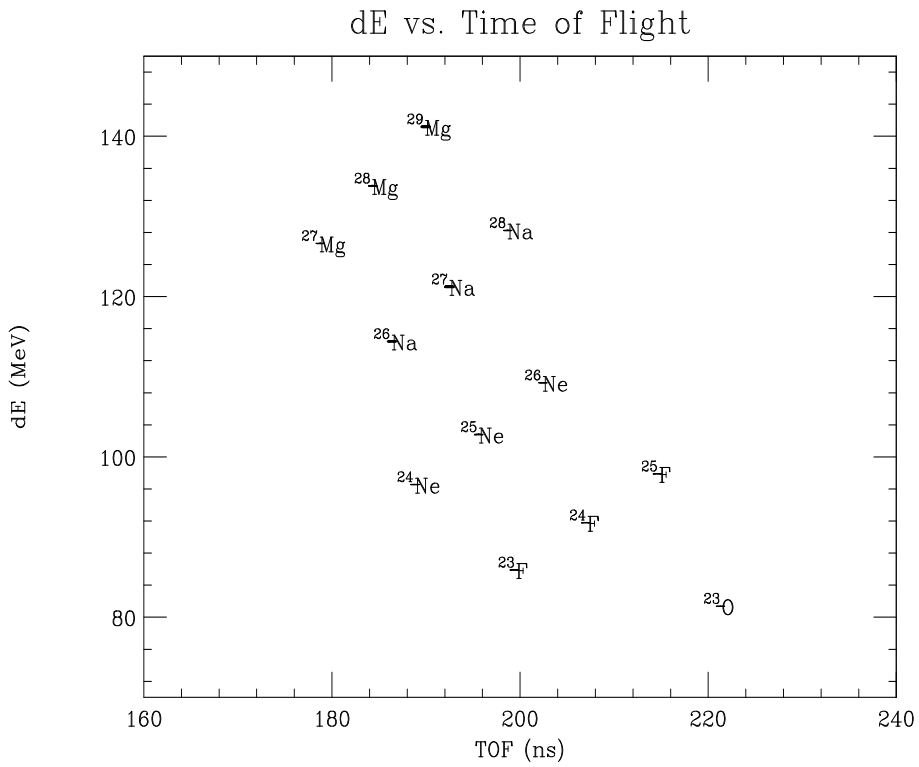

1.2.5 To calibrate RF1 and RF2 and to select real event

After RF signal is thinned because of high count rate, these are divided into two signals of RF1 and RF2 in order to get the data efficiently. These signals correspond to one cycle by one cycle. Thus, if the timing signal include proper range on one TDC, another TDC must be out of range. So, I have to reject the unproper signal.Following picture shows that and proper pulses set to come about 200ns.

calculation of intensity

Fragment	Rate (particle/s)	TOF(F0-F2) (ns)
^{25}Ne	6.223*10^3	201.4
^{26}Na	6.761*10^3	191.1
^{27}Na	8.963*10^3	197.4
^{28}Mg	5.013*10^3	189.0
^{29}Mg	9.808*10^3	194.8

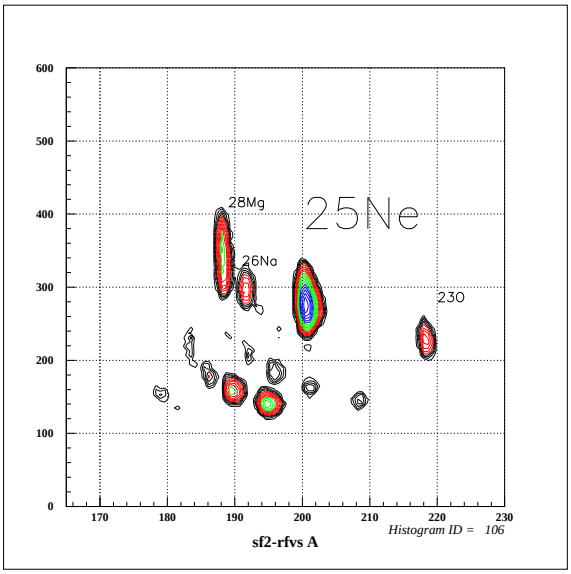

Figure 5: tof(ns) vs ΔE from experiment data

1.2.6 determination momentum of beam

Firstly, I introduce simply physics calculation to determine a beam momentum and β from measuring value in this experiment.

- B:the value of magnetic filed from NMR
- C:the velocity of the light
- ρ:the radius of curvature,3.6m at RIPS
- Z:the proton number of charged particle
- AMU:atomic mass unit
- P:momentum

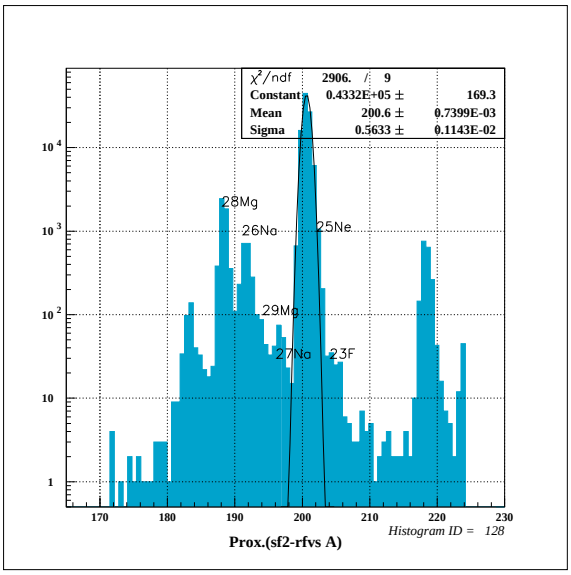

Figure 6: TOF (ns)

- E_{kin}:kinetic energy of the charged particle
- E_{total}:total energy of the charged particle

There are two NMR systems at D1 and D2 each other and this give me precise value of the magnetic field.

$$P = \frac{cB\rho Z}{A} \tag{5}$$

From momentum, you calculate kinetic energy.

$$E_{\mathrm{kin}} = \frac{P^2}{\sqrt{P^2 + AMU^2} + AMU} \tag{6}$$

$$E_{\mathrm{total}} = E_{\mathrm{kin}} + AMU \tag{7}$$

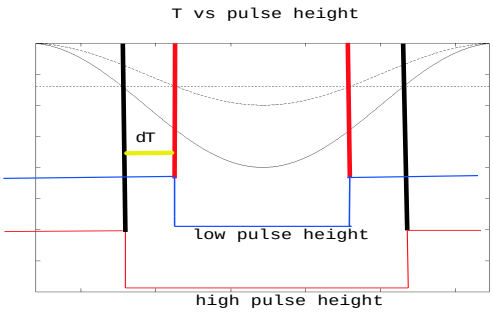

Figure 7: pulse height vs timing

$$\beta = \frac{P}{E} \tag{8}$$

From that, TOF is calculated in following.

- L: flight length

$$\mathrm{TOF} = \frac{\mathrm{L}}{\beta \mathrm{c}} \tag{9}$$

In above procedure, I calculate TOF from F0 to F2.Thus I determine absolute value. And I calculate beam momentum and β at D1,D2 by using magnetic filed value of NMR .

So, by using this value,I can select the real event on the experiment data .That is to say,the beta of unreal event is less than real beta in this set. Because this event is out of range at TDC and delayed about 80ns. In the next step,I analyze the momentum before the target. Though the beam line,many matter,F2PL, two PPACs,kapton miler and air which included from the end of the beam pipe to the target, included on that. I explain how to get this value in following sentence. The value after calculating above equation is corresponded to the central value of what I obtain from experimental data.To be from central value to outside that on a momentum distribution of that data, I can approximate β distribution on following equation.

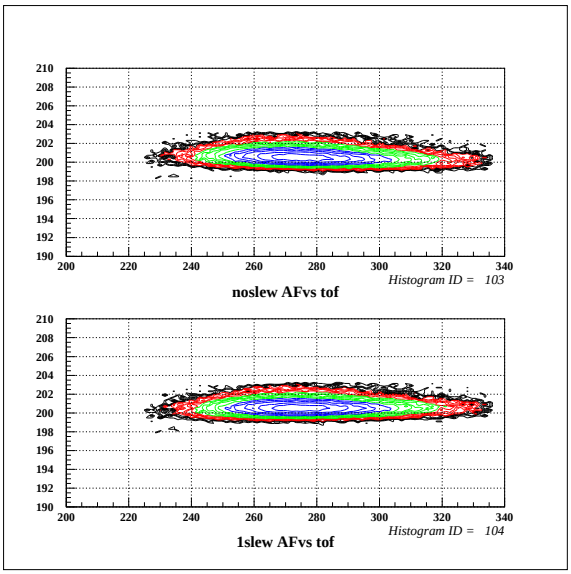

TOF(RF-SF2)

	σ
no slew	0.5061
one slew	0.4953

$$\beta_{\mathrm{D2}} = a + b\mathrm{TOF}_{\mathrm{F0-F2}} + \mathrm{cTOF}^2_{\mathrm{F0-F2}} \tag{10}$$

Similarly momentum is calculated. a,b,c is obtained by the calculation.

$$P_{\mathrm{aftermaterial}} = a + bP_{\mathrm{beforematerial}} + cP^2_{\mathrm{beforematerial}} \tag{11}$$

I check the value obtained from experiment data compared to the calculated value.

comparison

^{25}Ne

	calculation	exp
β_{D2}	0.3427	0.3425
$\frac{\mathrm{P}_{\mathrm{afttgt}}}{A}$	316.75[MeV]	316.7[MeV]
β_{afttgt}	0.32194	0.3220
$\frac{\mathrm{E}_{\mathrm{afttgt}}}{A}$	52.3803[MeV]	52.41[MeV]

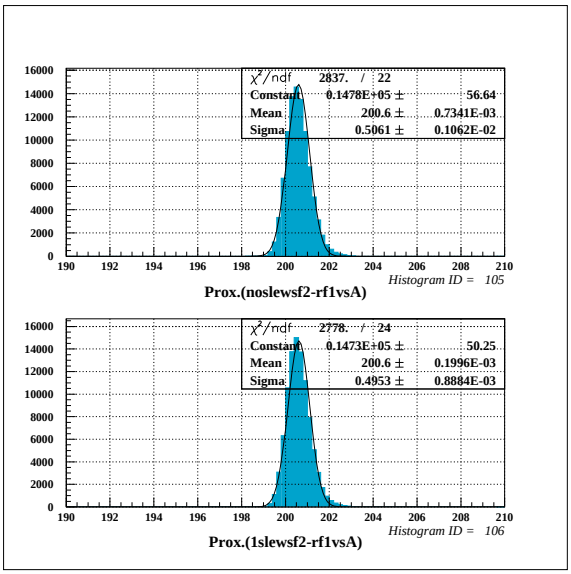

Figure 8: before slew correction and after correction

After rejecting unreal event by using comparison β between real event or not, I check the beam rate compared between before rejecting rate or after that. And I calculate the purity of ^{25}Ne of beam.

	count rate
RF1*^{25}Ne	47824
RF2*^{25}Ne	48146
βRF after selecting*^{25}Ne 60MeV/A at D2	95441
$(RF1 + RF2) \approx RF$	

$$purity = \frac{N_{^{25}\mathrm{Ne}}}{N_{\mathrm{total}}} = 79.6\%$$

N: all particle count rate at F2

1.2.7 particle identity of ^{26}Ne,$\Delta p/p = \pm 2\%$

This procedure of ^{26}Ne is same that of ^{25}Ne.

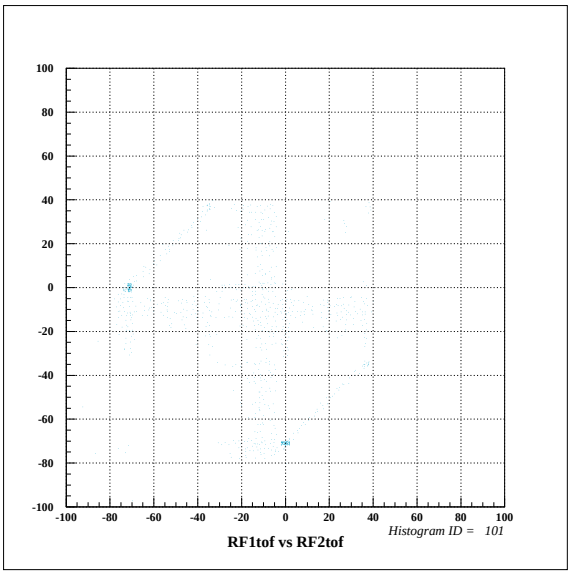

$$purity = \frac{N_{^{26}\mathrm{Ne}}}{N_{\mathrm{total}}} = 77.3\%$$

N:All particle count rate at F2

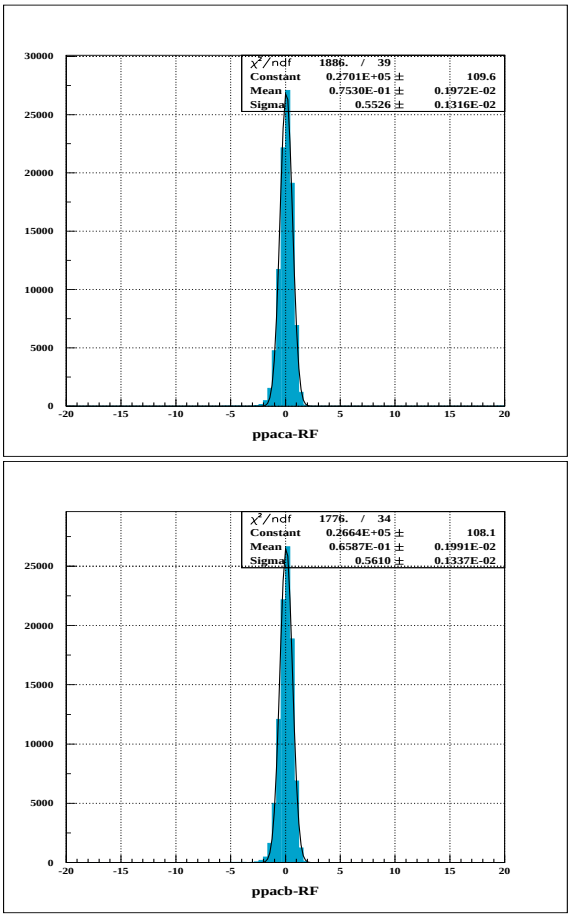

Figure 9: RF-SF2(TOF) and RF-PPACA,B(TOF)

1.2.8 momentum distribution of ^{26}Ne,$\Delta p/p = \pm 2\%$

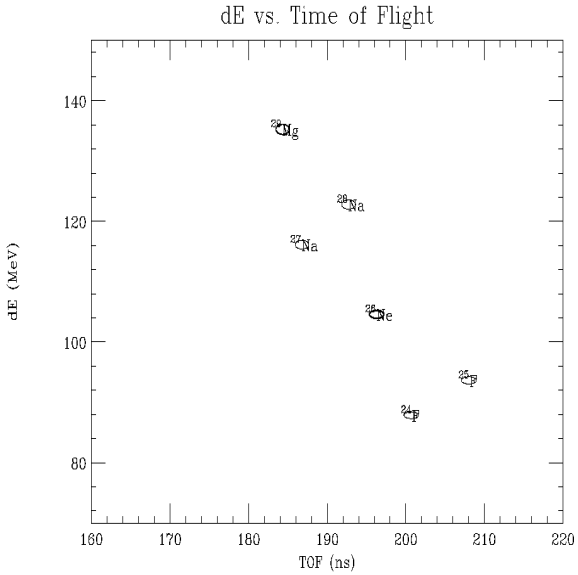

Figure 10: XIntensity TOF vs ΔE

calculation of intensity

Fragment	Rate (particle/s)	TOF (ns)
^{25}Ne	6.223*10^3	201.4
^{26}Na	6.761*10^3	191.1
^{27}Na	8.963*10^3	197.4
^{28}Mg	5.013*10^3	189.0
^{29}Mg	9.808*10^3	194.8

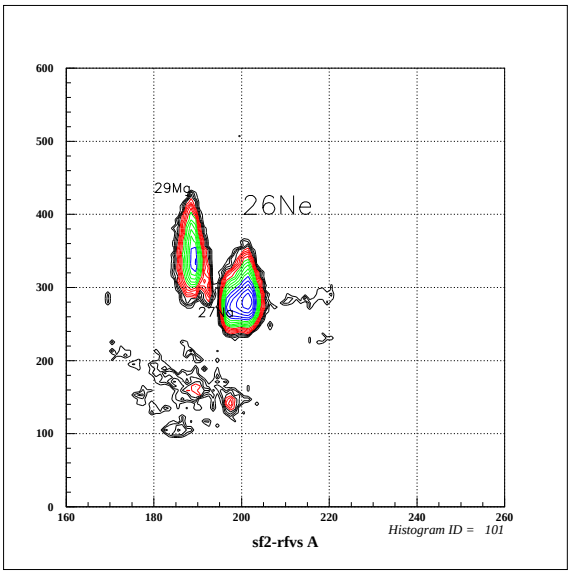

Figure 11: RF-SF2(TOF) VS A

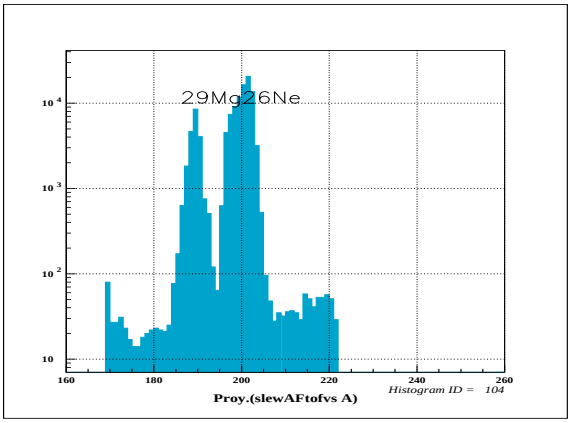

Figure 12: projection of timing

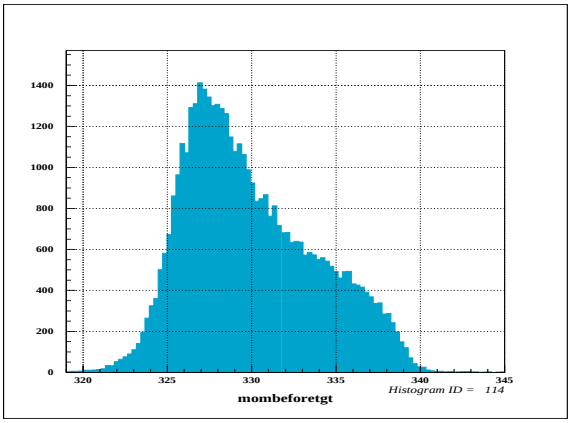

Figure 13: 26Ne momenutum before tgt

2 analysis of PPAC

2.1 principle

PPAC is composed of two cathode plates and one anode one. Cathode plate is strip type and from both side signals on one strip, projectile position of the beam can be read. To say that , I can measure the position by the time difference of both side signals. And accounting for above explanation, by using 2 plates,X strip and Y that,I can measure the angle of projectile beam and I can analyze momentum vector of that from beam momentum. Anode is used for measuring timing at projectile beam. But in this experiment, the time resolution is less than F2PL. So this value is not used on my analyses but only for reference. In this section, I analyze by using ^{26}Ne,$\Delta p/p = \pm 2\%$. I explain detail information for principle of PPAC in following.

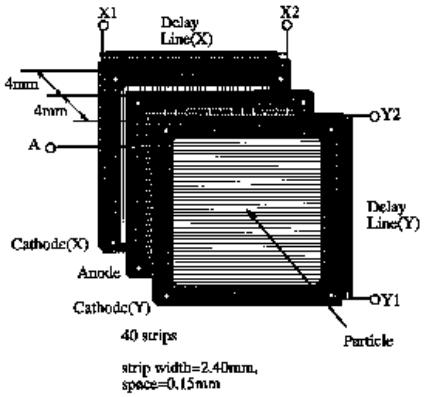

Figure 14: picture of the PPAC

$$\theta_{\mathrm{X}} = \tan^{-1}\frac{\mathrm{dX}}{\mathrm{Z_{PPACb}} - \mathrm{Z_{PPACa}}} \tag{12}$$

$$\theta_{\mathrm{Y}} = \tan^{-1}\frac{\mathrm{dY}}{\mathrm{Z_{PPACb}} - \mathrm{Z_{PPACa}}} \tag{13}$$

v:velocity of the current at strip of projectile beam detection
L:length of strip
x:position of projectile beam detection

$$(\mathrm{T_{left}} - \mathrm{T_{right}}) = \frac{\mathrm{x}}{\mathrm{v}} - \frac{\mathrm{L} - \mathrm{x}}{\mathrm{v}} \propto \mathrm{x} \tag{14}$$

2.2 efficiency

I calculate efficiency of PPAC.

$$(\mathrm{T_{left}} + \mathrm{T_{right}}) = \frac{\mathrm{x}}{\mathrm{v}} + \frac{\mathrm{L} - \mathrm{x}}{\mathrm{v}} = \mathrm{L/v} \propto \text{constant} \tag{15}$$

If signal is correct,sum of two signals is constant. Thus I analyze efficiency by using following equation.

$$efficiency(PPAC) = \frac{^{26}\mathrm{Ne_{F2}} \otimes (\mathrm{T_{right}} + \mathrm{T_{leght}} = \text{constant})_{\mathrm{PPAC}}}{^{26}\mathrm{Ne}} \tag{16}$$

efficiency	
PPACa	96.9%
PPACb	96.1%
PPACa⊗	93.4%

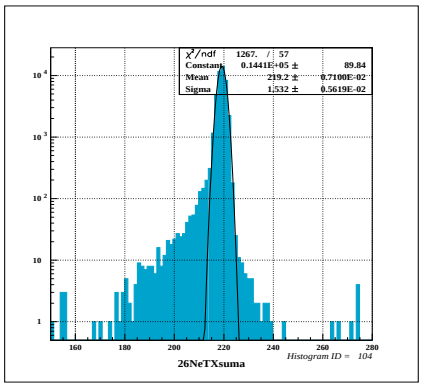

2.3 position and momentum distribution of projectile at target

From measured value, θ_x,θ_y distribution of projectile beam at target is evaporated.

$$\mathrm{X_{tgt}} = \mathrm{X_{PPACa}} + \mathrm{dX}\frac{\mathrm{Z_{tgt}} - \mathrm{Z_{PPACa}}}{\mathrm{Z_{PPACb}} - \mathrm{Z_{PPACa}}} \tag{17}$$

$$\mathrm{Y_{tgt}} = \mathrm{Y_{PPACa}} + \mathrm{dY}\frac{\mathrm{Z_{tgt}} - \mathrm{Z_{PPACa}}}{\mathrm{Z_{PPACb}} - \mathrm{Z_{PPACa}}} \tag{18}$$

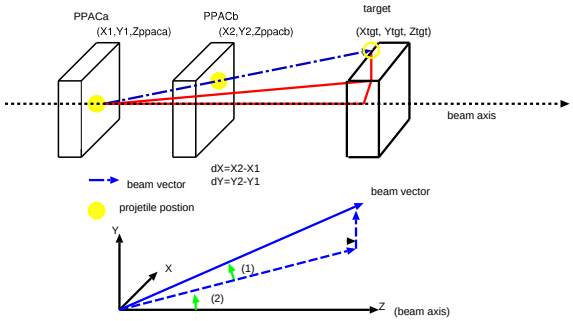

Figure 15: PPAC definition (1) θx (2)θy

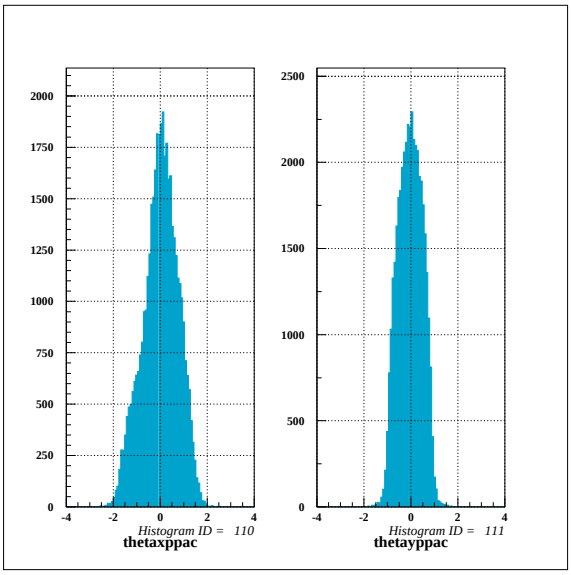

Figure 16: θ at target

2.4 momentum vector of projectile beam on target

I show the distribution of momentum of each axis of projectile beam. To measure that, I show procedure in below/

$$P_{\mathrm{X}} = P_{\mathrm{beam}} \frac{\tan\theta_{\mathrm{X}}}{\sqrt{1+\tan\theta_{\mathrm{X}}^2+\tan\theta_{\mathrm{Y}}^2}} \tag{19}$$

$$P_{\mathrm{Y}} = P_{\mathrm{beam}} \frac{\tan\theta_{\mathrm{Y}}}{\sqrt{1+\tan\theta_{\mathrm{X}}^2+\tan\theta_{\mathrm{Y}}{}^2}} \tag{20}$$

$$P_{\mathrm{Z}} = \sqrt{P_{\mathrm{beam}}^2 - P_{\mathrm{X}}{}^2 - P_{\mathrm{Y}}{}^2} \tag{21}$$

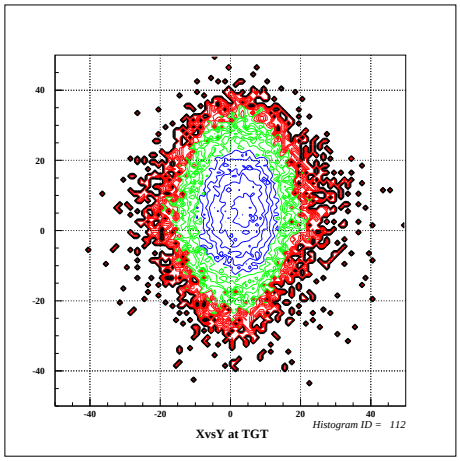

Figure 17: image on target

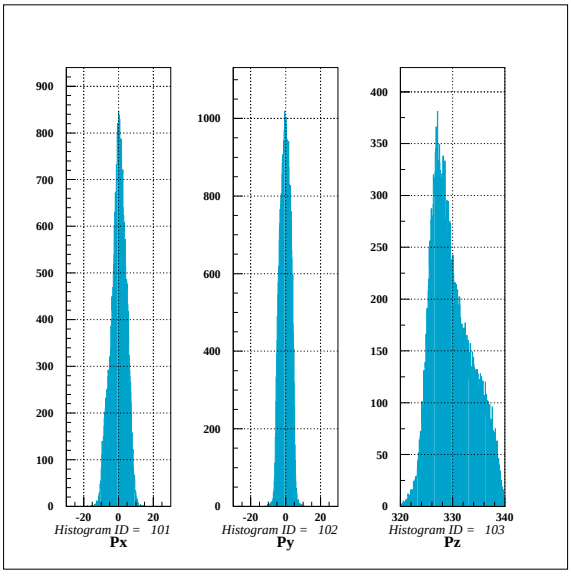

Figure 18: each momentum vector of the beam

3 silicon-strip detector

3.1 introduction

Particle identification of the fragments passing through the target was performed using four-layer-Si-strip-detectors composed of ΔE and E counters located at about 1.2 m downstream of the target. First two layers were composed of 8 Si detectors which were used for position detection. The position and intrinsic energy resolution of ΔE counters were about mm and 2%(FWHM),respectively. The last two layers was the E counter composed of 8 Si(Li) detectors with 3 mm thickness and has its intrinsic energy resolution of 3%(FWHM).

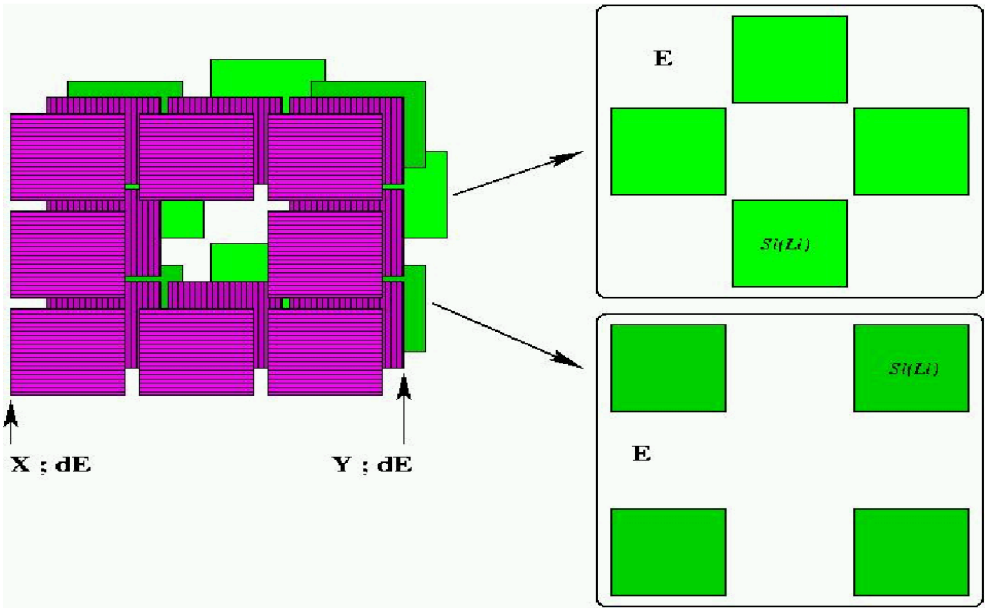

Figure 19: ssd parts

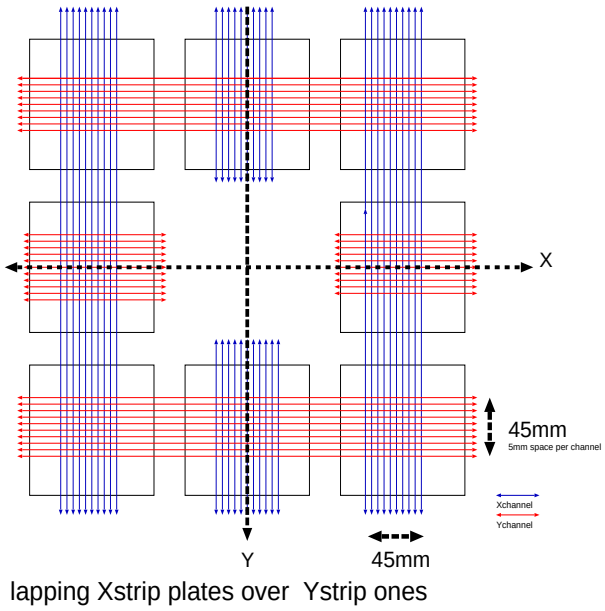

Figure 20: ssd facile picture of readout position

3.2 Energy Calibration ch⇒ MeV

The Energy calibration of each Silicon detectors was performed by using ^{25}Ne beam with 60 MeV/A, 55 MeV/A, and 50 MeV/A respectively. Figure shows the table which is correlation between ch and Energy[MeV].

table of calibration ^{25}Ne beam[MeV/A]				
E_{D2}	$\Delta E_{\mathrm{total}}$	deviation	E_{total}	deviation
60.04 MeV/Acal	10.16		50.0	
exp	10.03	-0.13	49.3	-0.7
55.41 MeV/A cal	11.19		43.91	
exp	11.20	-0.01	43.96	0.05
49.55 MeV/A cal	13.48		36.81	
exp	13.51	0.03	36.83	-0.02

3.3 How to identify the particle

$\Delta E_{\mathrm{total}}$is defined to the total energy loss of the fragments passing thought the ΔE counters and E_{total} is defined to the total kinetic energy of the fragments in front of the SSD counters. Therefore,

$$\Delta E_{\mathrm{total}} = \Delta E_{\mathrm{Xback}} + \Delta E_{\mathrm{Yback}} \tag{22}$$

$$E_{\mathrm{total}} = \Delta E_{\mathrm{total}} + E \tag{23}$$

- $\Delta E_{\mathrm{total}}$:the total energy of the $DeltaEcounters$
- $\Delta E_{\mathrm{Xback}}$,$\Delta E_{\mathrm{Yback}}$:the energy loss of the first layer and two layer respectively
- E_{total}:the total energy of the fragments
- E:the energy of the last E counter

In the energy loss of charged particle passing though the material,

$$\Delta E \simeq Z^2 \mathrm{TOF}^2 \tag{24}$$

- Z:the charge of the fragments
- TOF:the time of flight of the fragments

In the total energy of the fragments, this energy is classically equal to the kinetic energy.

$$E_{\mathrm{total}} \simeq \frac{A}{\mathrm{TOF}^2} \tag{25}$$

- A:the mass number of the fragments

Therefore,

$$E_{\mathrm{total}} \Delta E \simeq AZ^2 \tag{26}$$

This picture shows the identification of the fragments from ^{26}Ne incident beam at 58.7MeV/A.

To identify clearly, I did following way which is refereed from R.H.stokes et al,ReV.Sci.Instr.29.61(1958). Firstly the PID is defined following.

E_{total} is redefined following

$$E_{\mathrm{total}} = E + \frac{1}{2}\Delta E \tag{27}$$

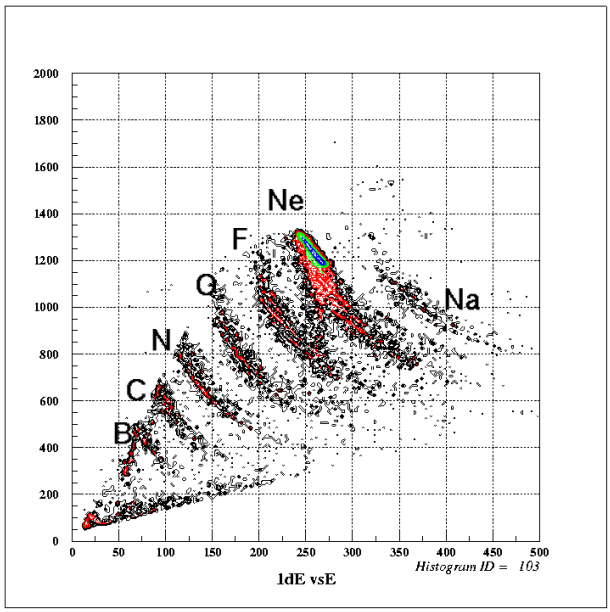

Figure 21: $\Delta Ecounters vs Ecounters$

Therefore,

$$\mathrm{PID} = \Delta E(E + \frac{1}{2}\Delta E)^a \simeq AZ^2 \tag{28}$$

a is parameter and the coefficient 1/2 means the mean energy loss of the $DeltaE$.

a≃0.75(in this analysis)

RUN	^{26}Ne+Pb	^{26}Ne+Al	^{26}Ne+emp
^{26}Ne	0.238	0.242	0.260
^{25}Ne	0.257	0.249	0.258
^{24}Ne	0.242	0.225	0.238
^{23}Ne	0.263	0.229	0.229
^{22}Ne	0.232	0.217	0.217
^{21}Ne	0.251	0.228	0.226
^{20}Ne	0.235	0.215	0.222

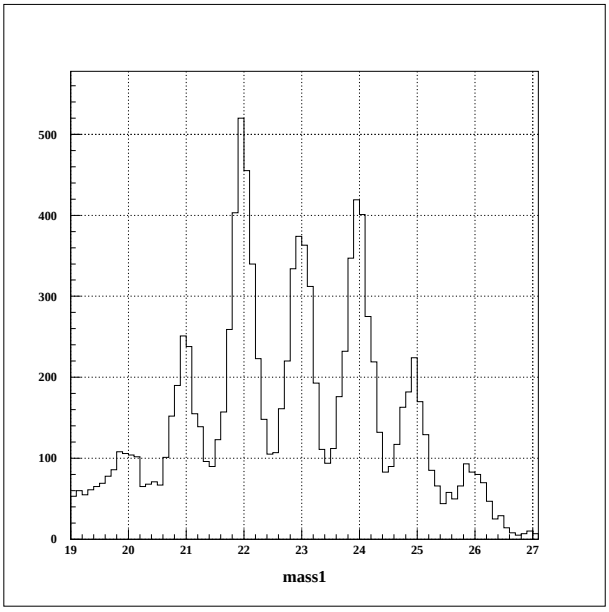

Figure 22: the distribution of ssd in Ne isotope at Pb target in beam⊗ssd⊗neutron

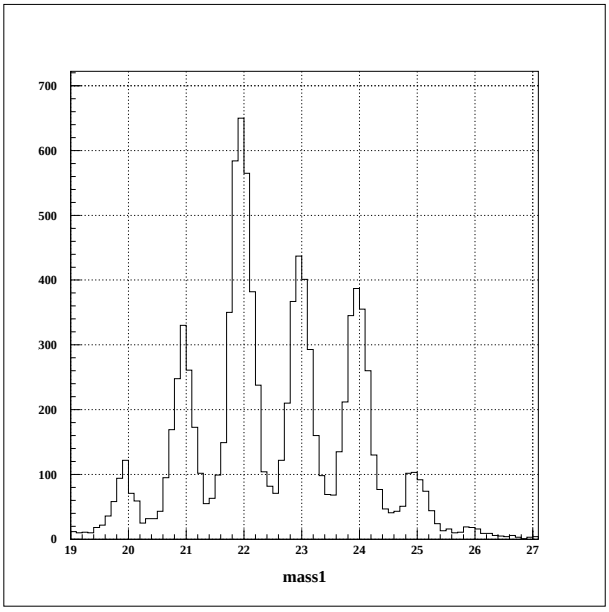

Figure 23: the distribution of ssd in Ne isotope at Al target in beam⊗ssd⊗neutron

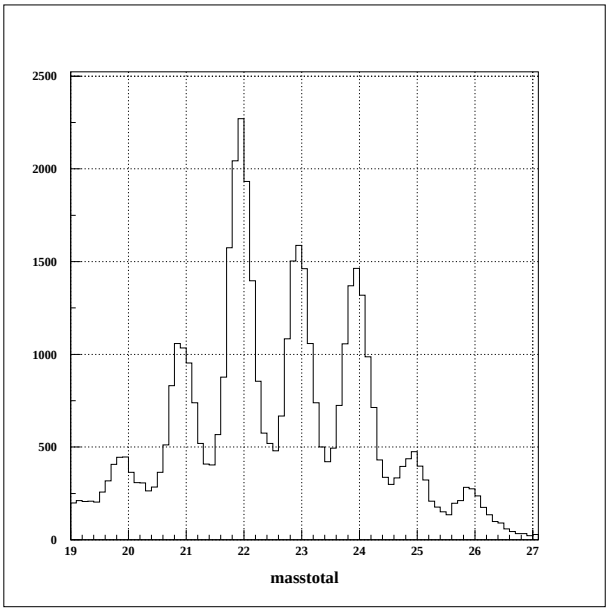

Figure 24: the distribution of ssd in Ne isotope at empty target in beam⊗ssd⊗neutron

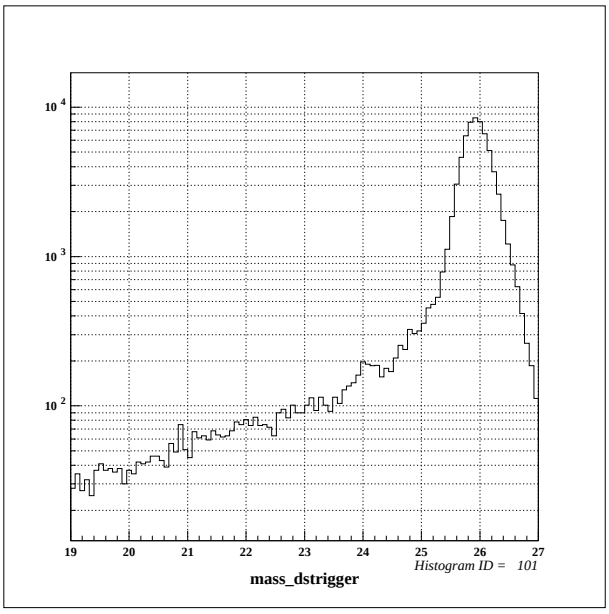

Figure 25: the distribution of ssd in Ne isotope at Pb target in beam trigger

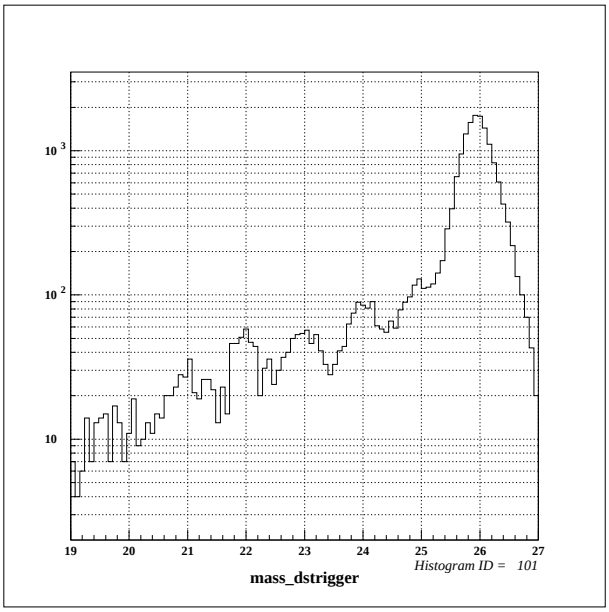

Figure 26: the distribution of ssd in Ne isotope at Al target in beam trigger

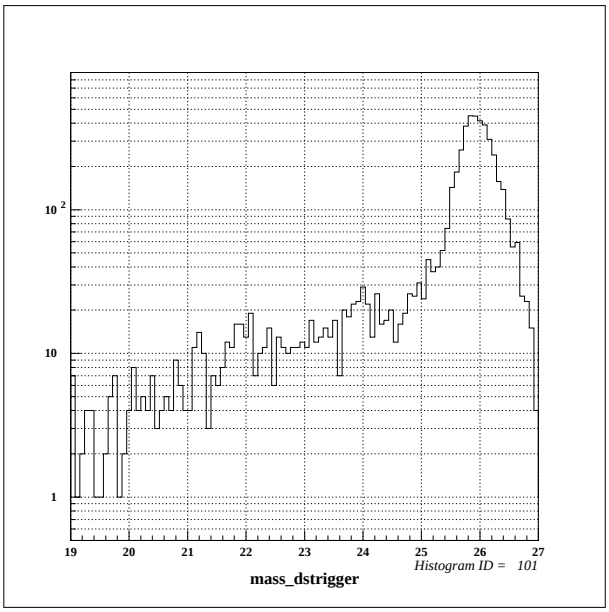

Figure 27: the distribution of ssd in Ne isotope at empty target in beam trigger

4 analysis of NaI

4.1 Energy calibration

The analog data of DALI were calibrated by using standard γ-ray sources of ^{137}Cs (662 keV),^{60}C0 (1173 keV and 1333 keV) and ^{22}Na(511 keV and 1275 keV). By fitting the energies with a linear function of channels ,calibration functions to convert channel to energy were deduced for each crystal of DALI. The energy calibration was checked by comparing the photo-peak positions in the energy spectra summed up for all the 152 NaI(Tl) scintillation detectors with the energies of the standard sources.

source	Energy(keV)	exp Energy(keV)	deviation(keV))
^{137}Cs	661.660	660.7	-0.3
^{60}C0	1173.237	1174.	0.6
	1332.501	1335.	2.5
^{22}Na	1274.532	1276.	1.5
	511	506.2	-4.8
^{9}Be+^{241}Am	4439.1	4428.	-11.1
	3928.1	3955.	27.
	3417.1	3402.	-15.

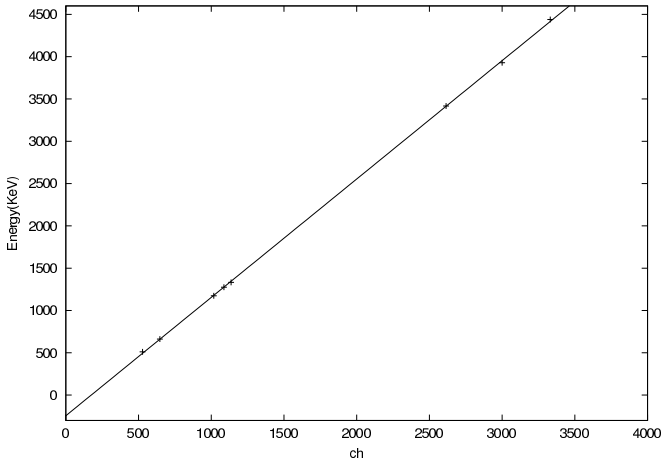

Figure 28: ch vs keV

function is

$$E_\gamma = \mathrm{a}E_{\mathrm{ch}} + \mathrm{b} \tag{29}$$

a and b are constant parameters.

4.2 timing calibration

I must arrange a timing of NaI detectors that these are same timing. This difference is caused by mainly different length of cables at each detectors.

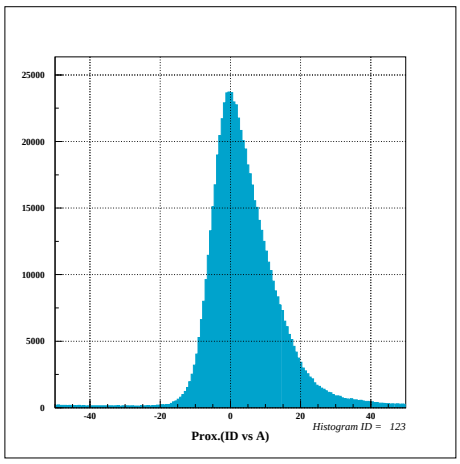

Figure 29: DALI timing (ns) after calibration

$$y = P1\exp[-\frac{(T - P2)^2}{2P3^2}] + P4 \tag{30}$$

$$T = T_{F2} - T_{Dali} \tag{31}$$

P4 is independent of a time.So this is interpreted as background components. So by rejecting this region which independent of physics that, S/N ratio will be up.

4.3 appendix of NaI

I used radioactive sources of ^{137}Cs,^{22}Na,^{60}Co and ^{241}Am-^{9}Be in this experiment.

4.3.1 ^{241}Am-^{9}Be

In that composition which include ^{241}Am and ^{9}Be, the following reaction is performing.

$$^{241}\mathrm{Am} \rightarrow \alpha + {}^{237}\mathrm{Np}$$
$$\alpha + {}^{9}\mathrm{Be} \rightarrow {}^{12}\mathrm{C}^{*} + \mathrm{n}$$

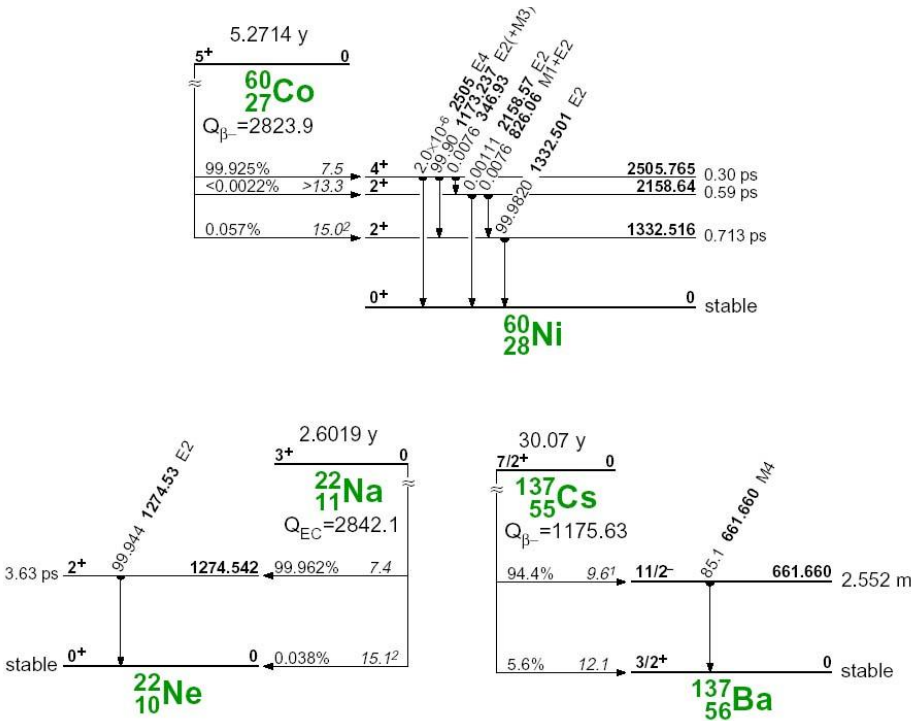

Figure 30: decay table

$^{12}C^*$ is immediately de-excited to the ground state though emitting γ-ray at 4.391 MeV. And in high energy γ-ray, pair productions are much arisen compared to the low energy.

$$\gamma \rightarrow e^- + e^+$$

e^+ is annihilated when this catches e^- within a matter. Two γ-ray,511 keV emitted after that. If NaI detector deposits energy from 2 γ-ray and $e-$ accompanied from pair creation , deposited energy is same asγ-ray energy from de-excited states. But if one γ-ray escapes from the detector and all other particle energy from pair creation is detected , NaI deposits

$$E_{\text{detected}} = E_\gamma - m_e c^2 \tag{32}$$

If two γ-ray escapes from that, NaI deposits

$$E_{\text{detected}} = E_\gamma - 2m_e c^2 \tag{33}$$

So from $^{12}C^*$, 3 type spectrum of energy ,4.4391 keV, 3.9281 keV and 3.417 keV is deposited by the NaI detector.

4.3.2 other radio active source

γ-ray is emitted from excited states of daughter nuclei after β decay table of radioactive sources in my experiment is shown following.

Only ^{22}Na decay though β minus decay

$$^{22}\text{Na} \rightarrow {}^{22}\text{Ne} + e^+ + \overline{\nu_e}.$$

So 511 keV γ-ray caused by this process.

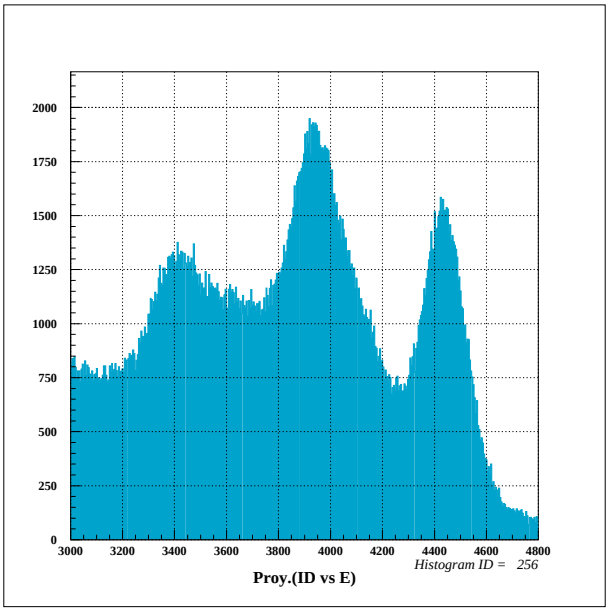

Figure 31: γ-ray from $^{12}C*$ and escape peaks

5 Doppler correction

5.1 introduction

In this experiment we detected γ-rays emitted from moving reaction products with a velocity v/c$\sim$0.32. Hence Doppler-shifted γ-ray energies were measured by the $\gamma - ray$ detectors. The transformation in the rest frame of the incident particle E_γ^{proj} and the γ -ray energy in the laboratory frame E_γ^{lab} is following.

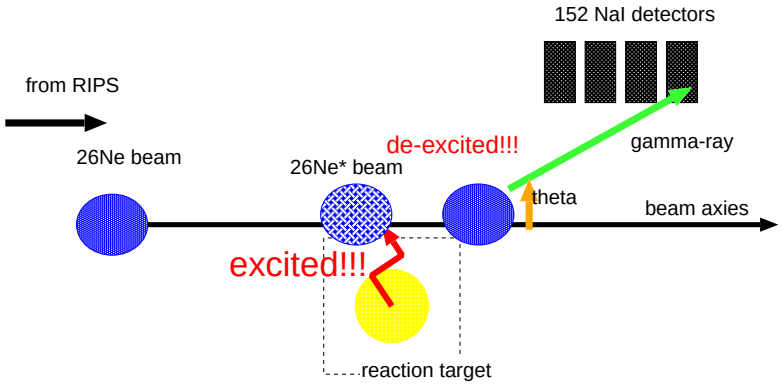

Figure 32: Schematic description of in-beam γ spectroscopy. The γ-ray detection angle with respect to the beam axis in the labratory frame θ.

$$\begin{pmatrix} E_\gamma^{\rm proj}/c \\ \mathbf{P}^{\rm proj} \end{pmatrix} = \begin{pmatrix} \gamma & -\beta\gamma \\ -\beta\gamma & \gamma \end{pmatrix} \begin{pmatrix} E_\gamma^{\rm lab}/c \\ \mathbf{P}^{\rm lab} \end{pmatrix}$$

- $E_\gamma^{\rm proj}$:γ energy in the rest frame of the incident particle
- $\mathbf{P}^{\rm proj}$:γ particle momentum in the rest frame of the incident particle
- $E_\gamma^{\rm lab}$:γ energy in the laboratory frame
- $\mathbf{P}^{\rm lab}$:γ particle momentum in the laboratory
- β:relativistic velocity
- γ:Loren factor $1/\sqrt{1-\beta^2}$

$$E_\gamma^{\rm proj}/c = \gamma E_\gamma^{\rm lab}/c - \gamma\beta\mathbf{P} \tag{34}$$

$$\beta = \beta\cos\theta \tag{35}$$

$$E_{\gamma}^{\mathrm{lab}} = h\nu \tag{36}$$

$$\mathbf{P} = \frac{h}{\lambda} = \frac{h\nu}{c} \tag{37}$$

$$\frac{P}{E_{\gamma}^{\mathrm{lab}}} = \frac{1}{c} \tag{38}$$

Therefore,

$$E_{\gamma}^{\mathrm{proj}} = E_{\gamma}^{\mathrm{lab}}\gamma(1 - \beta\cos\theta) \tag{39}$$

5.2 result

5.3 Energy resolution of the Doppler corrected γ-ray spectrum

Due to the finite accuracy of angular information and the velocity spread of the projectiles, the γ-ray energy peaks were broadened compared to the intrinsic energy resolution of the detectors. Based on equation, the resolution E_{γ}^{proj} is approximated,

$$(\frac{\Delta E_{\gamma}^{\mathrm{proj}}}{E_{\gamma}^{\mathrm{proj}}})^2 = (\frac{\beta\sin\theta_{\gamma}^{\mathrm{lab}}}{1-\beta\cos\theta_{\gamma}^{\mathrm{lab}}})^2(\Delta\theta_{\gamma}^{\mathrm{lab}})^2 + (\frac{\beta\gamma^2(\beta-\cos\theta_{\gamma}^{\mathrm{lab}})}{1-\beta\cos\theta_{\gamma}^{\mathrm{lab}}})^2(\frac{\Delta\beta}{\beta})^2 + (\frac{\Delta E_{\gamma}^{\mathrm{lab}}}{E_{\gamma}^{\mathrm{lab}}})^2 \tag{40}$$

From the correlation between energy and σ, the intrinsic energy resolution of the detectors is introduced in following.

$$\sigma = 1.9\sqrt{E} - 26.97 \tag{41}$$

The energy resolutions are evaluated using realistic condion, β of 0.32 and γ of 1.06 with $\Delta\theta_{\mathrm{max}}$ of 20 degrees in labratory frame of 90 degrees and $\Delta theta_{\mathrm{min}}$ of 0 degrees in labratory frame of 0 degrees respectively, $\Delta\beta/\beta$ of 11.5% including the energy loss in the secondary target.

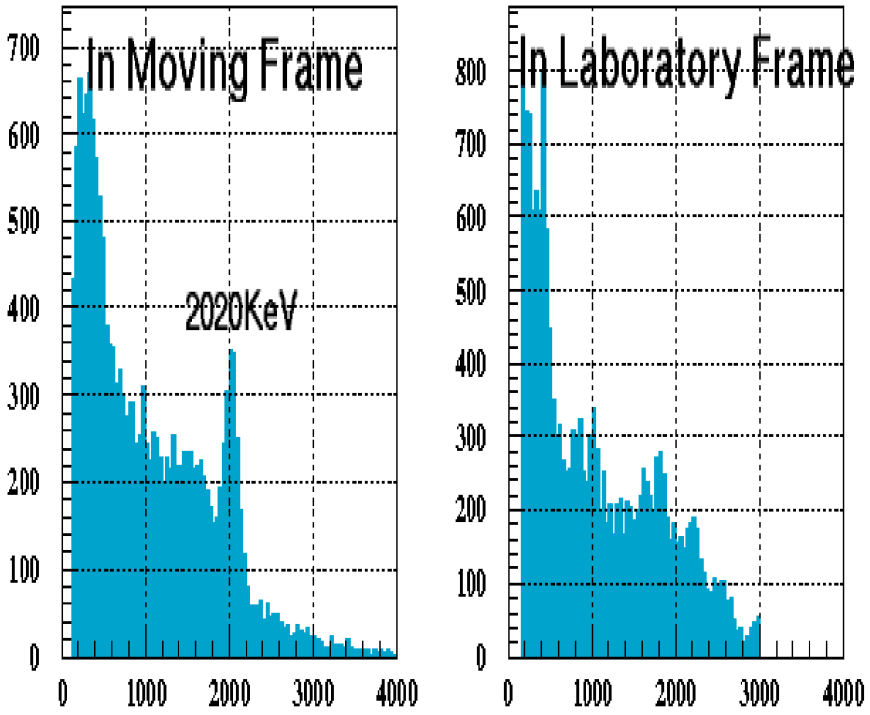

Figure 33: Energy spectrum of γ rays detected in coincidence with the ^{26}Ne reaction products.(right)Energy spectrum in laboratory frame.(left)Doppler-corrected γ rays energy spectrum with β=0.32. The peaks at 2020 keV is clearly seen while they are vague in right indicating a good quality of the Doppler correction.

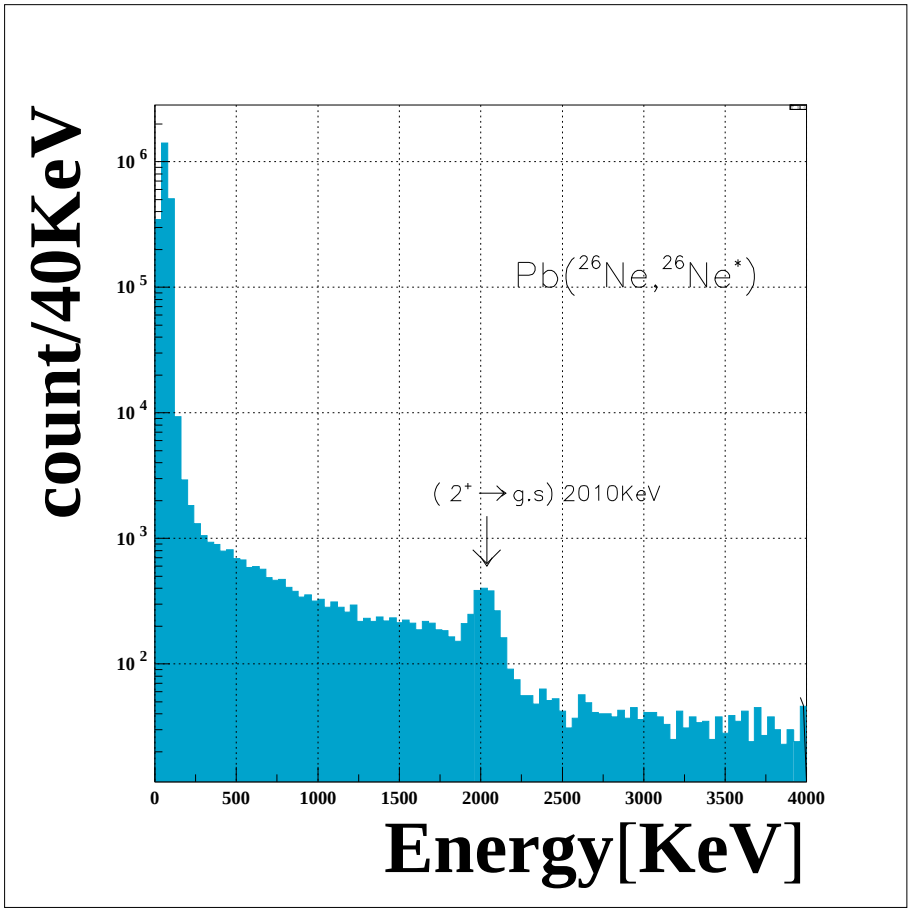

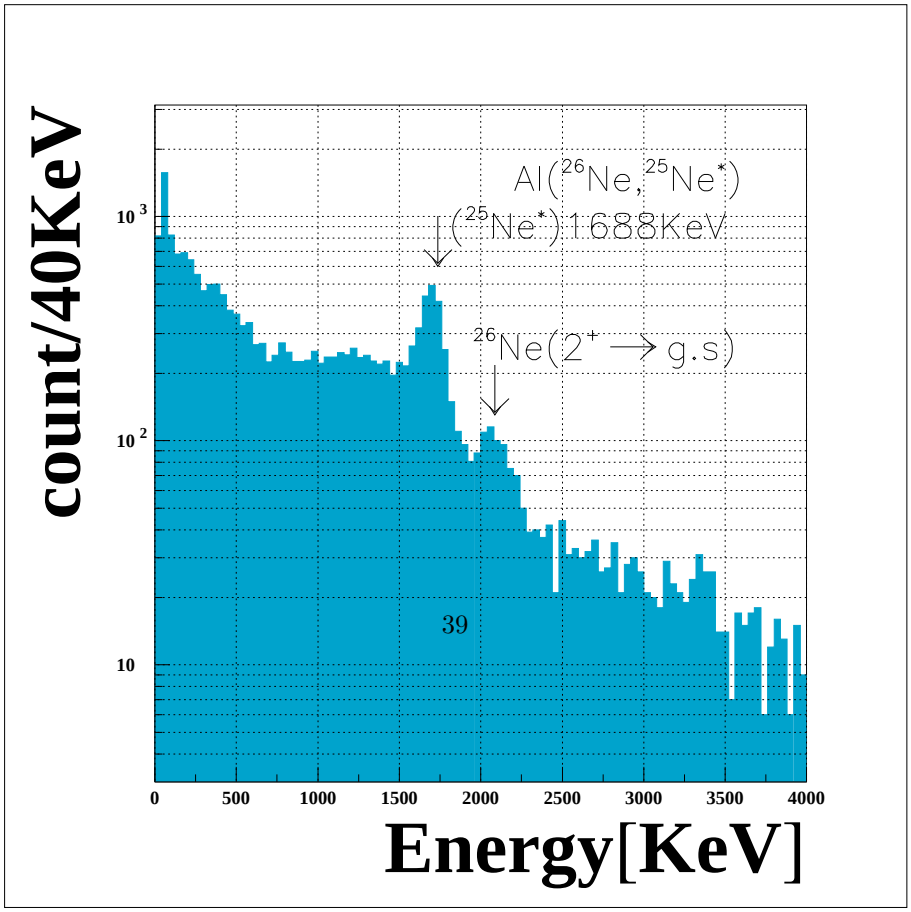

Figure 34: Gamma-ray energy spectra obtained in coincidence with the reaction products 26Ne,^{25}Ne.

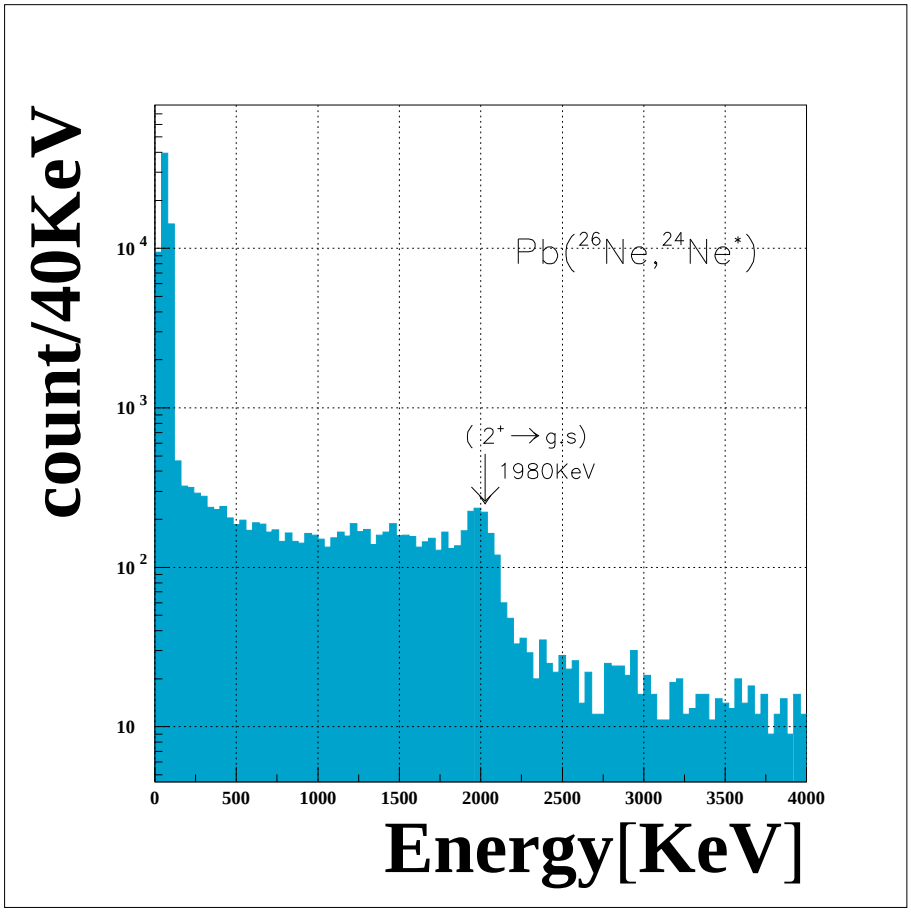

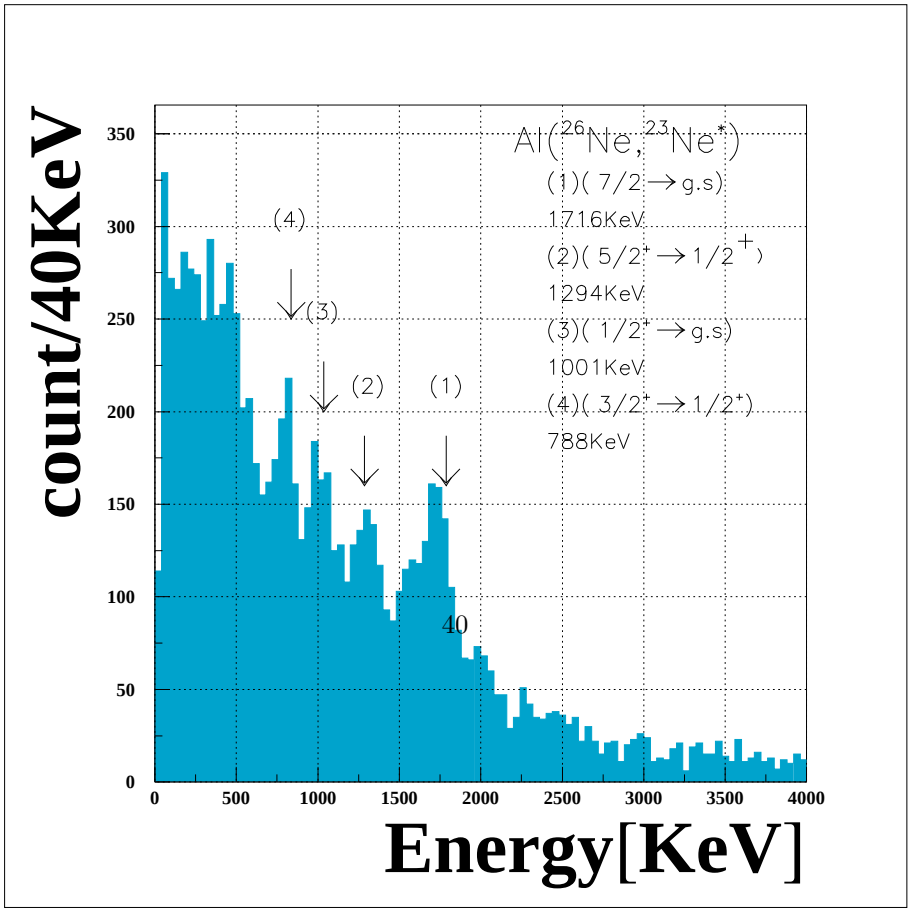

Figure 35: Gamma-ray energy spectra obtained in coincidence with the reaction products 24Ne,^{23}Ne.

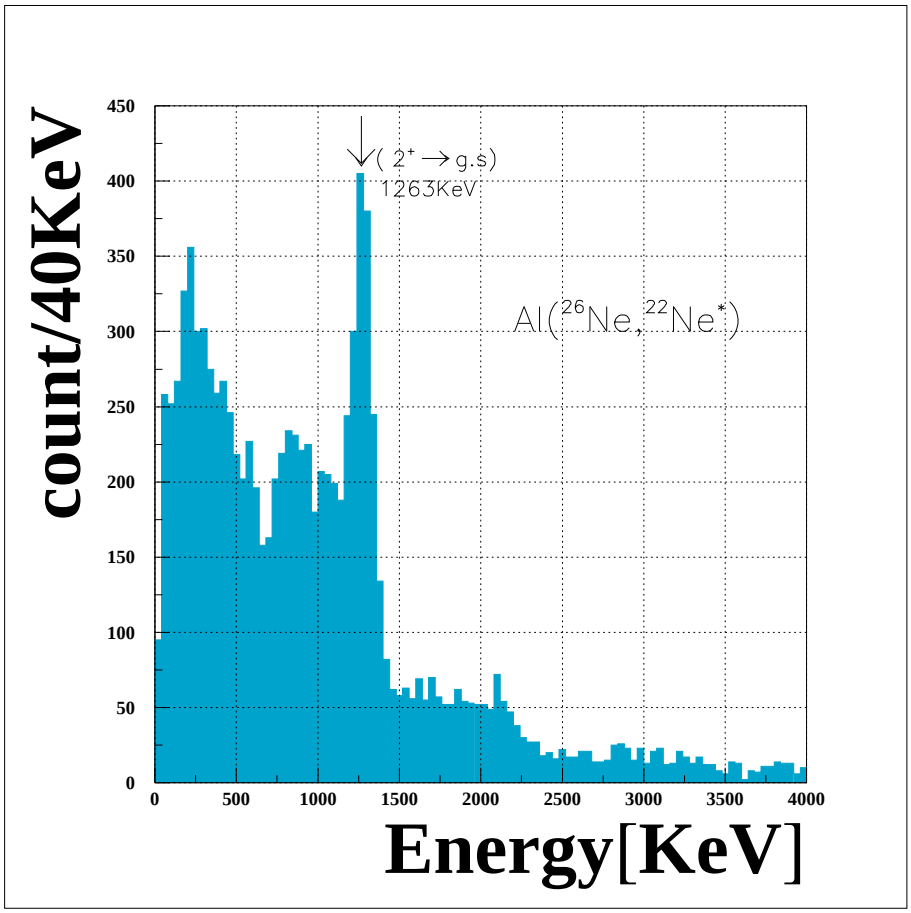

Figure 36: Ne fragments gamma ray spectrum

Figure 37: Gamma-ray energy spectra obtained in coincidence with the reaction products 22Ne.

fragment	E(exp)[keV]	σ	E(previous)[keV]	deviation[keV]	state
^{26}Ne	2020	109	2020	0	$(2^+ \rightarrow g.s)$
^{25}Ne	1688	89	1702	-14	unkown
^{24}Ne	1978	98	1981.6	3.6	$2^+ \rightarrow g.s$
^{23}Ne	1716	134	1701	15	$7/2 \rightarrow g.s$
	1294	170	1298	-4	$5/2^+ \rightarrow 1/2^+$
	1001	159	1017	-16	$1/2^+ \rightarrow g.s$
	785	120	805	-20	$3/2^+ \rightarrow 1/2^+$
^{22}Ne	1263	85	1274.5	-11	$2^+ \rightarrow g.s$
	848	171	-	-	-

Figure 38: Gamma-ray energies of Ne isotopes from A of 26 to A of 22. The energies deduced in the present work are compared with the literature values.

source	^{137}Cs	^{60}C		^{22}Na		Am-Be		
Energy[keV]	661	1173	1332	511	1274	3417	3928	4428
σ[keV]	26	32	36	25	36	84	105	95

Figure 39: The energy resolution of obtained value in standard gamma souce.

fragment	^{26}Ne	^{25}Ne	^{24}Ne	^{22}Ne
Energy[keV]	2020	1688	1978	1263
$\sigma[exp]$[keV]	109	89	98	85
$\sigma[calc]$[keV]	121	102	119	78

Figure 40: Energy resolution σ of obtained Doppler correted spectrum. The σ values in the present work are compared with the calcurated value.

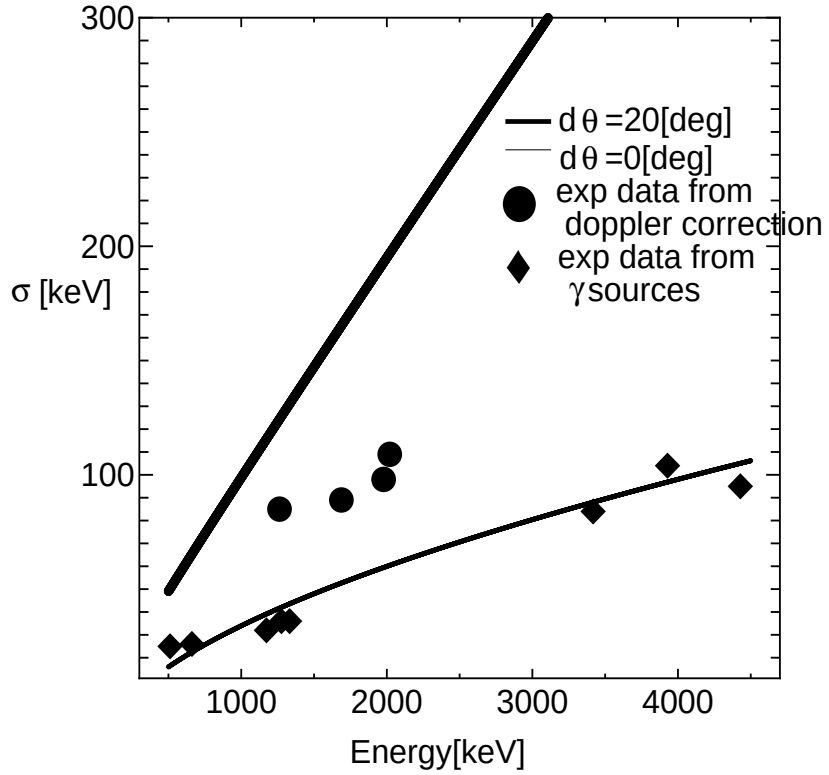

Figure 41: Energy resolutions for the function of energy of γ-ray emitted from moving souces .

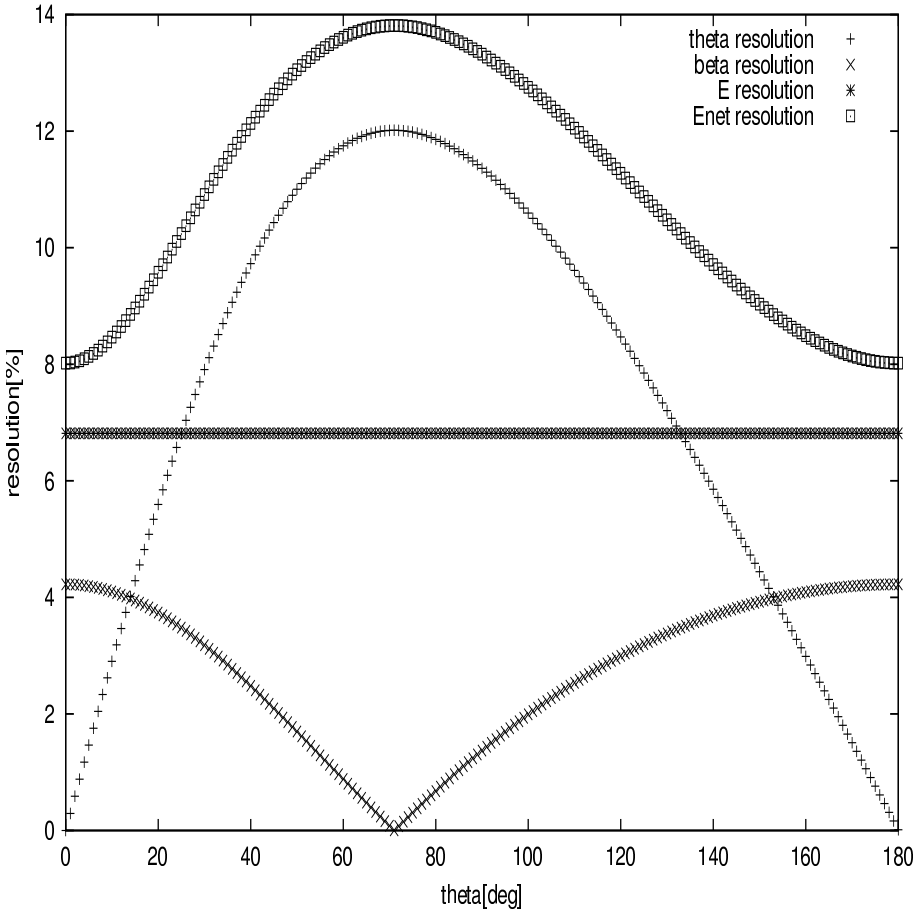

Figure 42: Energy resolutions for 2 MeV γ-ray emitted from moving souces with v/c$\approx$0.32

6 efficiency calculation

6.1 calculation

I used the radio active source data to estimate the efficiency. The ^{137}Cs,^{22}Na and^{60}Co was used. Efficiency is estimated following equation.

$$\epsilon = \frac{Yield_{\text{detected}}}{Yield_{\text{emission}}} \tag{42}$$

source	^{137}Cs	^{22}Na	^{60}Co
Energy[keV]	661	1173,1332	511,1274
intensity(T=0)[kBq]	46.6	359	41.2
half time($t_{1/2}$)[year]	30.07	2.6019	5.2714
emission probability[%]	0.8521	0.999,0.9998	0.9994

Firstly, I calculate the efficiency from the source run.

source	^{137}Cs	^{60}C		^{22}Na	
Energy[keV](exp)	661	1173	1332	511	1274
$Yiled_{\text{emission}}$	4.25×10^{7}	3.82×10^{7}	3.82×10^{7}	2.20×10^{8}	1.10×10^{8}
$Yiled_{\text{detected}}$	3.17×10^{4}	1.96×10^{5}	1.77×10^{5}	6.40×10^{5}	1.74×10^{5}
$Yiled_{\text{detected}}$(calibrated)	1.35×10^{6}	6.31×10^{6}	5.70×10^{6}	7.80×10^{7}	2.14×10^{7}
efficiency[%]	31.7	16.5	14.9	35.4	19.4

$Yiled_{\text{detected}}(calibrated)$ means

$Yiled_{\text{detected}}$(calibrated)=$\frac{\text{ungatedevent}}{\text{gatedevent}}$ * (DS − Dalitrigger)*$Yiled_{\text{detected}}$

- DS-dali trigger:Down scale factor
- $\frac{\text{ungatedevent}}{\text{gatedevent}}$:livetime of Dali trigger
- $Yield_{511} = 2 * Yield_{1274\text{KeV}}$ in ^{22}Na

I calculated the efficiency by using the **GEANT** code which reproduces well the measured efficiencies.

Energy[keV]	661	1173	1332	511	1274	E(2020kev; $2^{+} \rightarrow$ g.s)
efficiency[%](calc)	31.0	20.2	18.5	38.4	19.1	13.6

Figure shows plot of photo-peak efficiencies as a function of γ-ray energies.The solid line was calculated by the **GEANT** code. For 2 MeV, efficiencies was estimated attained to be about 18 % and this curve is within the 15%ddeviation. This concluded that this systematic error $\Delta\epsilon$ is 15%.

In 2 Mev γ-ray, I estimated 13.9 % of the efficiency and determined 15% of the systematic error from this figure.

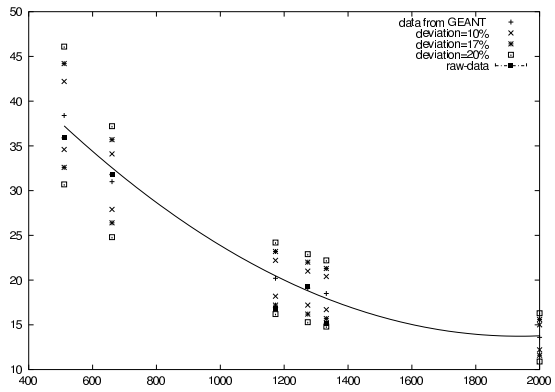

Figure 43: comparison calculation data from raw data

6.2 appendix

$$A = -\tau \frac{dN}{dt} = \tau N \tag{43}$$

$$N(t) = N(0)e^{-t/\tau} \tag{44}$$

$$\tau = t_{1/2} \log 2 \tag{45}$$

- A:the number of decay
- τ:decay constant
- $t_{1/2}$:half time
- $N(t)$:Yield

7 Cross section

7.1 formula

Cross section σ is given by

$$\sigma_{\mathrm{reaction}} = \frac{\mathrm{N_{reaction}}}{\mathrm{N_{beam}}} \frac{\mathrm{A}}{\mathrm{tN_A}} \tag{46}$$

- $\sigma_{\mathrm{reaction}}$:cross section of one events
- N_{reaction}:the number of one reaction events
- N_B:the number of the secondary beam,^{26}Ne
- A[g/mol]:the mass number
- t[g/cm^2:thickness of the target
- N_A[1/mol]:Avogadro's number

In this experiment,

- A:208[Pb]
- t:0.230[g/cm^2]

$$\frac{\mathrm{A}}{\mathrm{tN_A}} = 149.64 * 10^{-27} m^2 \tag{47}$$

- A:27[Al]
- t:0.130[g/cm^2]

$$\frac{\mathrm{A}}{\mathrm{tN_A}} = 34.48 * 10^{-27} m^2 \tag{48}$$

$$\sigma = \frac{\mathrm{N_{fragment}}}{\mathrm{N_{beam}}} \frac{\mathrm{A}}{\mathrm{tN_A}} \epsilon \tag{49}$$

$\mathrm{N_{beam}}$ is given by

$$\mathrm{N_{beam}} = (\mathrm{DS} - \mathrm{factor}) * \mathrm{N_{^{26}Ne}} * (\mathrm{LiveTime})_{\mathrm{DS}} \tag{50}$$

- ϵ:the correction of the detectors
- DS-factor:down scale factor
- $(\mathrm{LiveTime})_{\mathrm{DS}}$:the live time of the down scale beam trigger

DS-factor and Live time is

$$(\mathrm{DS-factor}) = \frac{\mathrm{N_{beam}(scaler)}}{\mathrm{N_{DS}(scaler)}} \tag{51}$$

$$(\mathrm{LiveTime})_{\mathrm{DS}} = \frac{(\mathrm{DS-beam_{(raw-data)}})}{(\mathrm{DS-beam_{(scaler)}})} \tag{52}$$

$\mathrm{N_{fragment}}$ is given by
in the case of beam⊗ssd⊗neutron trigger

$$\mathrm{N_{fragment}} = \mathrm{N_{raw-data}} * (\mathrm{Livetime})_{\mathrm{b\otimes s\otimes n}} * \epsilon(\mathrm{acceptance}) \tag{53}$$

- $(\mathrm{Livetime})_{\mathrm{b\otimes s\otimes n}}$:the live time of the beam ⊗ ssd ⊗ neutron trigger

$$(\mathrm{LiveTime})_{\mathrm{b\otimes s\otimes n}} = \frac{\mathrm{N_{b\otimes s\otimes n}(raw-data)}}{\mathrm{N_{b\otimes s\otimes n}(scaler)}} \tag{54}$$

ϵ_γ(acceptance) is given by montecalro simulation.
in the case of beam⊗ssd⊗DALI trigger

$$\mathrm{N_{fragment}} = \mathrm{N_\gamma} * (\mathrm{Livetime})_{\mathrm{b\otimes s\otimes d}} * \epsilon(\mathrm{efficiency}) \tag{55}$$

$$(\mathrm{LiveTime})_{\mathrm{b\otimes s\otimes d}} = \frac{\mathrm{N_{b\otimes s\otimes d}(raw-data)}}{\mathrm{N_{b\otimes s\otimes d}(scaler)}} \tag{56}$$

- N_γ:the number of the photon peak
- $(\mathrm{Livetime})_{\mathrm{b\otimes s\otimes d}}$:the live time of the beam ⊗ ssd ⊗ dali
- $\epsilon_{\mathrm{efficiency}}$:efficiency of the DALI including acceptance of the geometry

ϵ is given by GEANT3 code.

RUN	^{26}Ne+Pb	^{26}Ne+Al	^{26}Ne+emp
Ungated Trigger(scaler)	14852201	4920463	1551938
Accepted Trigger(scaler)	13598070	4738277	152043
beam⊗SSD⊗DALI(scaler)	11084097	2136137	378380
beam⊗SSD⊗DALI(raw-data)	10038675	1952605	328419
beam⊗SSD⊗NEUT(scaler)	3306474	2166475	547899
beam⊗SSD⊗NEUT(raw-data)	2982517	1979953	472618
DS-Beam(scaler)	1578423	1755869	822505
DS-Beam(raw-data)	1443494	1630666	725995
Beam	789451741	878002704	411256850
Live Time(all)	0.92	0.96	0.98
Live Time(bsd)	0.91	0.91	0.87
Live Time(bsn)	0.90	0.91	0.86
Live Time(ds)	0.91	0.93	0.88
DS-factor	500	500	500
^{26}Ne(raw-data)*(livetime)	501886813	553961828	272365909

Figure 44: The table of each trigger event

7.2 the list of trigger event and livetime

After subtracting empty run

7.3 cross-section

Cross section table is following. The unit is mb.

The $E(2020;2^+)$ of the ^{26}Ne is following.

RUN	^{26}Ne+Pb	^{26}Ne+Al
photo-peak$E(2020\text{keV}; 2^+)$	2495	2111
fitting error	55	55
statics error	50	46
ϵ efficiency	13.6%	13.6%
$\Delta\epsilon/\epsilon$	15%	15%
ϵ acceptance		
σ cross-section(mb)	60(9))	11(2)

7.4 appendix

How to estimate the value of the error.

$$\sigma_{\text{reaction}} = \frac{\text{N}_{\text{frag}}}{\text{N}_{\text{B}}} \frac{\text{A}}{\text{tN}_{\text{A}}} \tag{57}$$

- $\sigma_j$reaction:cross section of one events

RUN	^{26}Ne+Pb(live time)	^{26}Ne+emp(live time)	^{26}Ne+emp(live time)
^{25}Ne	11510(12789)	16010(17593)	2426(2821)
^{24}Ne	33470(37189)	32340(35538)	7963(9259)
^{23}Ne	31910(3546)	29650(32582)	8225(9564)
^{22}Ne	41010(45567)	31810(34956)	11090(12895)
^{21}Ne	17370(19300)	14260(15670)	5058(5881)
^{20}Ne	4373(4859)	3853(4234)	1406(1635)

Figure 45: The counts of Ne isotope from A of 26 to A of 20 at each target in coincidence with neutron.

RUN	^{26}Ne+Pb(error)	^{26}Ne+Al(error)
^{25}Ne	7591(216)	11856(234)
^{24}Ne	20127(357)	16706(331)
^{23}Ne	17832(351)	13130(329)
^{22}Ne	21804(403)	8728(352)
^{21}Ne	8462(293)	3708(253)
^{20}Ne	1846(243)	909(162)

Figure 46: The counts of Ne isotope from A of 26 to A of 20 after subtracting empty target run at Pb and Al target in coincidence with neutron.

- N_{fragment}:the number of each fragments number
- N_B:the number of the secondary beam,^{26}Ne
- A[g/mol]:the mass number
- t[g/cm^2:thickness of the target
- N_A[1/mol]:Avogadro‘s number

$\Delta\sigma$ is introduced by following

$$\Delta\sigma = \sqrt{(\frac{\Delta N_{\text{frag}}}{N_{\text{frag}}})^2 + (\frac{\Delta\epsilon_{\text{frag}}}{\epsilon_{\text{frag}}})^2 + (\frac{\Delta N_B}{N_B})^2} \tag{58}$$

Subtracting empty target run from each target run produced the error of the each target run with error of the empty run.

In empty run

ds-beam(factor=500)

RUN	^{26}Ne+Pb(live time)	^{26}Ne+Al(live time)	^{26}Ne+emp(live time)
^{25}Ne	847(931)	827(889)	184(209)
^{24}Ne	449(493)	732(787)	154(175)
^{23}Ne	630(692)	414(445)	56(64)
^{22}Ne	353(388)	172(185)	73(83)
^{21}Ne	149(164)	380(409)	20(23)

Figure 47: The counts of Ne isotope from A of 26 to A of 20 at each target onbeam trigger.

RUN	^{26}Ne+Pb(error)	^{26}Ne+Al(error)
^{25}Ne	545(121)	464(127)
^{24}Ne	171(66)	431(90)
^{23}Ne	575(65)	316(63)
^{22}Ne	235(55)	16(53)
^{21}Ne	122(68)	362(322)

Figure 48: The counts of Ne isotope from A of 26 to A of 20 after subtracting empty target run at Pb and Al target on beam trigger.

$$N_{\text{emp}} = x \pm \Delta x \tag{59}$$

In target run

$$N_{\text{tgt}} = y \pm \Delta y \tag{60}$$

In empty subtraction,

$$F = N_{\text{tgt}} - C1 * N_{\text{emp}} \tag{61}$$

Therefore

$$\Delta N_{\text{frag}} = \Delta F \tag{62}$$

- C1:the coefficient in normalizing target statics

RUN	^{26}Ne+Pb(error)	^{26}Ne+Al(error)
^{25}Ne	23(3.0)	7(1.3)
^{24}Ne	60(2.1)	10(0.7)
^{23}Ne	53(1.0)	8(0.3)
^{22}Ne	65(1.3)	5(0.1)
^{21}Ne	25(0.4)	2(0.1)
^{20}Ne	8(0.2)	1(0.01)

Figure 49: The cross section table at each target in coincidence with neuron.

Ds-beam cross-section is following. The unit is mb.

RUN	^{26}Ne+Pb(error)	^{26}Ne+Al(error)
^{25}Ne	813(452)	144(128)
^{24}Ne	255(60)	134(438)
^{23}Ne	857(97)	98(20)
^{22}Ne	350(135)	5(1)
^{21}Ne	182(40)	113(31)

Figure 50: The cross section table at each target on beam trigger.

$$\Delta F = \sqrt{(\frac{\delta F}{\delta x})^2(\Delta x)^2 + (\frac{\delta F}{\delta y})^2(\Delta y)^2} \tag{63}$$

$$\frac{\delta F}{\delta x} = 1 \tag{64}$$

$$\frac{\delta F}{\delta y} = C1 \tag{65}$$

Therefore

$$\Delta F = \sqrt{(\Delta x)^2 + (\Delta y * C1)^2} \tag{66}$$

- ϵ:acceptance of the ssd calculating doing now
- N_B:the number of the secondary beam,^{26}Ne
- N_B:the statics error of the photon peak number
- $\Delta N^{\rm sta}_{\rm frag}$:the statics error of the photon peak number

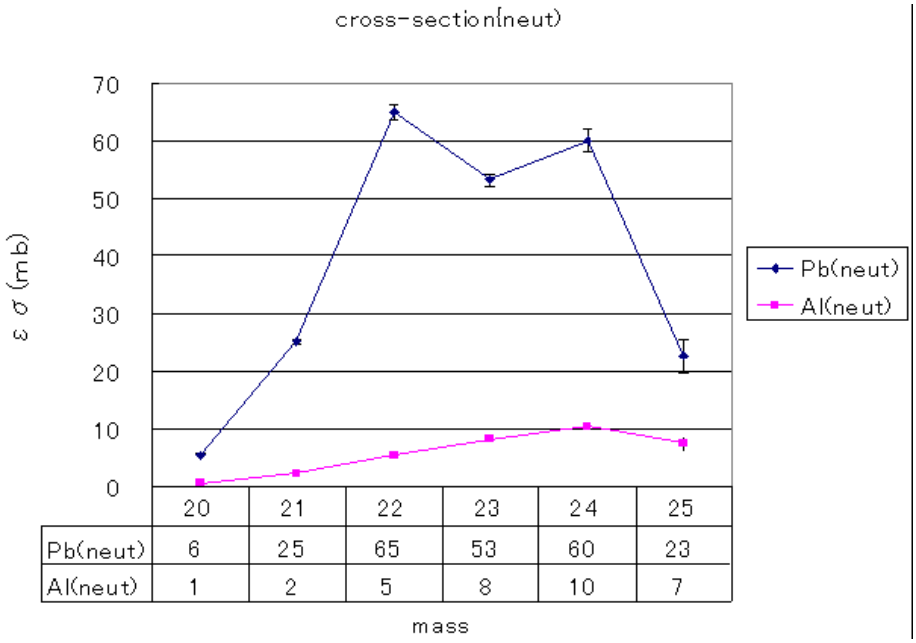

	20	21	22	23	24	25
Pb(neut)	6	25	65	53	60	23
Al(neut)	1	2	5	8	10	7

- $\Delta N_{\rm frag}^{\rm fit}$:the fitting error of the photon peak

In the γ-ray spectrum case, the estimate of the error is following.

$$\sigma = \frac{\mathrm{N}_\gamma}{\mathrm{N}_{\rm beam}} \frac{\mathrm{A}}{\mathrm{t}\mathrm{N}_{\rm A}} \tag{67}$$

Therefore,

$$\frac{\Delta\sigma}{\sigma} = \sqrt{(\frac{\Delta N_\gamma}{N_\gamma})^2 + (\frac{\Delta\epsilon_\gamma}{\epsilon_\gamma})^2 + (\frac{\Delta N_B}{N_B})^2} \tag{68}$$

$$\Delta N_\gamma = \sqrt{(\Delta {N^{\rm sta}}_\gamma)^2 + (\Delta N_\gamma^{\rm fit})^2} \tag{69}$$

- σ:cross section
- N_γ:the number of the photon peak
- ϵ:efficiency of the DALI including acceptance of the geometry
- N_B:the statics error of the photon peak number

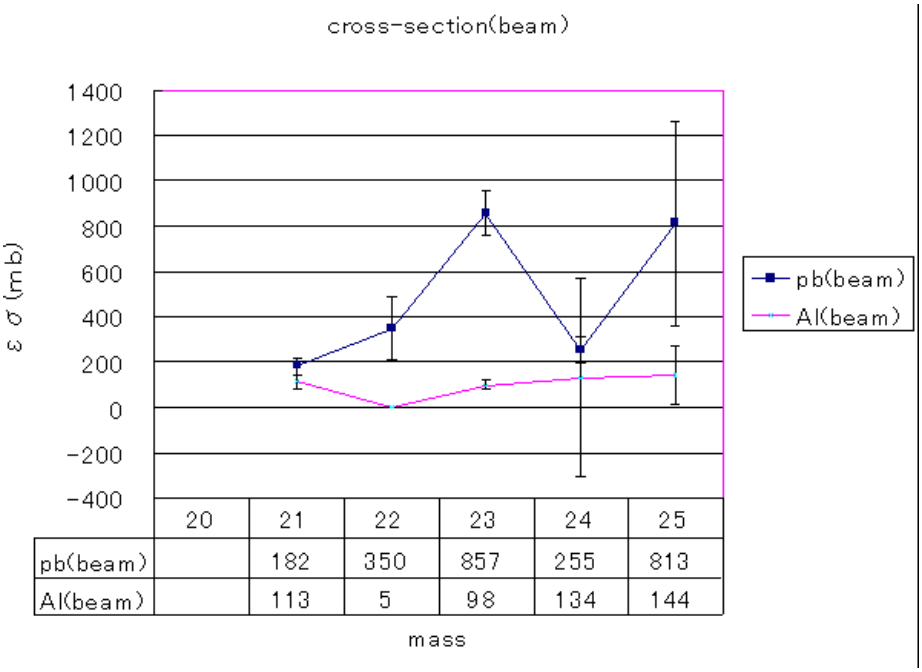

- $\Delta N_{\gamma}^{\mathrm{sta}}$:the statics error of the photon peak number
- $\Delta N_{\gamma}^{\mathrm{fit}}$:the fitting error of the photon peak